Phytochemistry 143 (2017) 170–179

Contents lists available at ScienceDirect

Phytochemistry

journal homepage: www.elsevier.com/locate/phytochem

Idesia polycarpa (Salicaceae) leaf constituents and their toxic effect on *Cerura vinula* and *Lymantria dispar* (Lepidoptera) larvae

Felix Feistel, Christian Paetz, Sybille Lorenz, Franziska Beran, Grit Kunert, Bernd Schneider*

Max Planck Institute for Chemical Ecology, Hans-Knöll-Straße 8, Beutenberg Campus, D-07745, Jena, Germany

ARTICLE INFO

Article history:
Received 8 June 2017
Received in revised form
1 August 2017
Accepted 7 August 2017

Keywords:
Cerura vinula
Idesia polycarpa
Lymantria dispar
Populus nigra
Salicaceae
Phenolic glycosides

ABSTRACT

Phytochemical investigation of *Idesia polycarpa* (Salicaceae) resulted in the structure elucidation of nine previously undescribed phenolic natural products along with six known compounds. The compounds are structurally related to salicinoids that are known defense compounds from *Salix* and *Populus* species. The *I. polycarpa* diet was toxic, as shown in feeding experiments with larvae of *Lymantria dispar*, an herbivorous broadleaf tree generalist insect, and with larvae of *Cerura vinula*, a specialist adapted to poplar. The survival rate and mass gain of larvae was significantly lower when they fed on *I. polycarpa* leaves, compared to larvae fed on *Populus nigra* leaves. Potential reasons for the poor performance of both herbivores on *I. polycarpa* leaves are discussed.

1. Introduction

Idesia polycarpa is a deciduous tree of the Salicaceae family and the only species of the monotypic genus *Idesia*. Originally native to East Asia, it is now a common ornamental tree worldwide. It forms edible orange berry-like fruits that remain on the tree after leaf senescence. The fruits have been phytochemically investigated, and a variety of compounds, including phenolic glycosides such as idesin, idescarpin (**15**), idesolide, salirepin and phenazine derivatives, were isolated (Chou et al., 1997; Kim et al., 2005; Moritake et al., 1987). Most previous studies focused on pharmaceutical applications. Extracts of *I. polycarpa* were reported to show antioxidant, anti-inflammatory and depigmenting effects (Baek et al., 2006; Ye et al., 2014), inhibition of platelet aggregation (Chou et al., 1997), apoptosis induction (Jung et al., 2010), nitric oxide production (Hwang et al., 2012) and anti-adipogenic activity (Hwang et al., 2012; Lee et al., 2013). The ecological function of compounds of *I. polycarpa*, however, has not yet been investigated. Except for the above-mentioned compounds from the fruit and some from the seed oil (Guo et al., 2012), natural products from other parts of this plant are unknown. Although extracts of *Idesia* seeds and leaves have been traditionally applied as insecticides in the Koreas, surprisingly, the underlying chemistry is still unknown (Kim, 1996; Kim et al., 2005). We isolated the major UV-active metabolites from leaf extracts and elucidated their chemical structures. Most of the compounds show a great similarity to phenolic defense compounds reported from other Salicaceae species, such as *Populus* and *Salix*. We also investigated anti-herbivory properties of *Idesia* leaves in feeding experiments with the larvae of the herbivorous generalist (*Lymantria dispar*) and the specialist (*Cerura vinula*) (both Lepidoptera) which is adapted to thrive on different Salicaceae species including *P. nigra* (Hintze-Podufal, 1970; Robinson et al., 2010).

2. Results and discussion

2.1. Isolation and structure elucidation

An extract of lyophilized leaves of *I. polycarpa* was prepared as described in Experimental. Subfractions of the extract were separated by high performance liquid chromatography coupled to solid phase extraction (HPLC-SPE). The separation resulted in isolation of 15 compounds with nine to-date-unknown natural products (**1**–**9**). Six compounds were formerly described as icaraside B2 (**10**), 4-(*E*)-

* Corresponding author.
E-mail address: schneider@ice.mpg.de (B. Schneider).

http://dx.doi.org/10.1016/j.phytochem.2017.08.008
0031-9422/

p-coumaroyl-glucopyranose (**11**), isograndidentatin (**12**), 1-*O*-(2-hydroxyphenyl)-4-*O*-(*E*)-*p*-coumaroyl-*β*-glucopyranose (**13**), idescarpaside (**14**) and idescarpin (**15**) (Fig. 1). Spectroscopic data from the new compounds are shown in Tables 1 and 2 and in Experimental. Data from formerly described but insufficiently characterized compounds are provided in Experimental and Supplementary Data.

The molecular formula of compound **1** was determined to be $C_{17}H_{22}O_9$ by its molecular ion obtained in high resolution electrospray mass spectrometry (HRESIMS) at *m/z* 369.1185 $[M\text{-}H]^-$ (calcd for $C_{17}H_{21}O_9$, *m/z* 369.1191). The ^1H NMR data of compound **1** showed signals (Table 1) assignable to three different structural units with a total of 17 protons. The low-field range of the ^1H NMR spectrum showed a four-spin system (AA'XX') with signals at δ_H 6.84 (H-3″/5″) and δ_H 7.51 (H-2″/6″), both with a coupling constant $^3J_{HH} = 8.7$ Hz, a characteristic of a 1,4-disubstituted aromatic ring. The corresponding ^{13}C chemical shifts were determined by a cross-signal in the ^1H-^{13}C heterocorrelation single quantum coherence (HSQC) spectrum to be δ_C 116.7 (C-3″/5″) and δ_C 131.1 (C-2″/6″), respectively. The structure of the 1,4-disubstituted aromatic ring was corroborated by the ^1H-^{13}C heteronuclear multiple-bond correlation (HMBC) spectrum. The $^3J_{CH}$ correlation of H-2″/6″ with δ_C 161.3 determined C-4″ to be an oxygenated carbon atom. Another HMBC correlation from H-2″/6″ to a methine carbon atom at δ_C 147.1 (δ_H 7.70, $^3J_{HH} = 15.9$ Hz) marked the first position (C-7″) of a π-system tethered to C-1″ (δ_C 127.0) of the aromatic ring. A cross-signal in the ^1H-^1H correlation spectroscopy (^1H-^1H COSY) spectrum identified the second methine proton (H-8″) of the π-system at δ_H 6.40 ($^3J_{HH} = 15.9$ Hz, which is characteristic of an *E*-configuration). The ^{13}C chemical shift value of the corresponding carbon atom (δ_C 114.6, C-8″) was assigned by a ^1H-^{13}C HSQC correlation. Both methines showed long-range CH-correlations to a quaternary carbon atom at δ_C 168.4, which is assignable to C-9″ and, together with the signals of the aromatic ring and the double bond, indicated

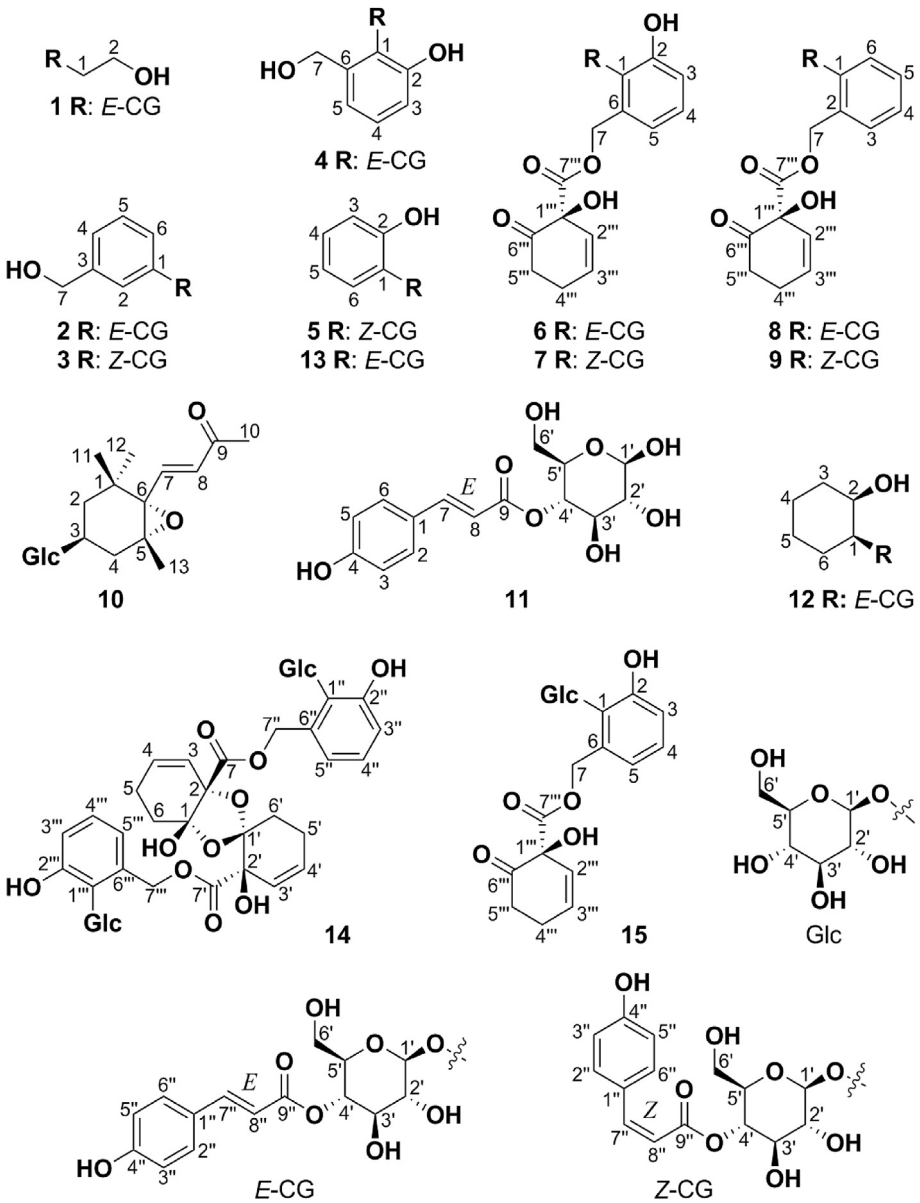

Fig. 1. Phenolic glycosides isolated from leaves of *I. polycarpa*. Compounds **1**–**9** are new natural products. The substituents are abbreviated as follows: *β*-glucose (Glc), 4-(*E*)-*p*-coumaroyl-*β*-glucopyranose (*E*-CG) and 4-(*Z*)-*p*-coumaroyl-*β*-glucopyranose (*Z*-CG).

Table 1
^{1}H NMR (700 MHz) and ^{13}C NMR data (175 MHz) of compounds **1**–**5** in MeOH-d_4.

Position	**1**		**2**		**3**		**4**		**5**	
	δ_H mult. (*J* in Hz)	δ_C	δ_H mult. (*J* in Hz)	δ_C	δ_H mult. (*J* in Hz)	δ_C	δ_H mult. (*J* in Hz)	δ_C	δ_H mult. (*J* in Hz)	δ_C
1a	3.69 *m*	72.3		159.2		159.0		144.3		146.3
1b	3.98 *m*									
2	3.73 *m*	62.2	7.13 *s*	116.1	7.12 *s*	116.2		150.6		147.7
3				144.5		144.2	6.85 *d* (8.0)	117.2	7.19 *dd* (1.3/8.0)	118.9
4			7.02 *m*	121.8	7.01 *d* (7.9)	121.8	7.03 *dd* (8.0/7.5)	126.7	6.78 *ddd* (1.5/7.6/8.0)	120.8
5			7.27 *dd* (7.8/7.8)	130.2	7.26 *dd* (7.9/8.0)	130.4	6.89 *d* (7.5)	121.0	6.92 *ddd* (1.3/7.6/8.0)	124.8
6			7.03 *m*	116.5	7.01 *d* (8.0)	116.5		136.5	6.84 *dd* (1.5/8.0)	117.0
7a			4.56 *s*	64.8	4.58 *s*	64.8	4.64 *d* (12.7)	60.4		
7b							4.81 *d* (12.7)			
1′	4.38 *d* (7.8)	104.3	4.99 *d* (7.8)	102.2	4.96 *d* (8.0)	102.3	4.68 *d* (8.0)	106.7	4.81 *d* (8.4)	104.1
2′	3.34 *dd* (9.0/7.8)	75.2	3.58 *dd* (7.8/9.3)	74.9	3.57 *dd* (8.0/9.2)	74.9	3.64 *dd* (8.0/9.4)	75.5	3.61 *dd* (8.4/9.4)	74.9
3′	3.65 *dd* (9.0/9.0)	75.4	3.75 *dd* (9.3/9.6)	75.6	3.70 *dd* (9.2/9.1)	76.2	3.72 *dd* (9.4/9.3)	75.6	3.70 *dd* (9.4/9.6)	75.1
4′	4.85 *m*	72.3	4.95 *dd* (9.6/9.9)	72.1	4.94 *dd* (9.1/10.0)	71.7	4.94 *dd* (9.3/9.7)	72.0	4.96 *d* (9.6/9.6)	71.6
5′	3.53 *m*	76.1	3.71 *ddd* (9.9/6.0/2.0)	76.1	3.70 *ddd* (2.0/6.5/10.0)	76.1	3.58 *ddd* (2.0/6.2/9.7)	76.5	3.62 *ddd* (2.0/5.8/9.6)	76.1
6′a	3.54 *dd* (5.6/12.6)	62.3	3.67 *dd* (12.6/6.0)	62.1	3.65 *dd* (6.5/12.3)	62.2	3.63 *dd* (2.0/12.2)	62.2	3.58 *dd* (5.8/12.1)	61.9
6′b	3.62 *dd* (2.0/12.6)		3.58 *dd* (12.6/2.0)		3.57 *dd* (2.0/12.3)		3.58 *dd* (6.2/12.2)		3.67 *dd* (2.0/12.1)	
1″		127.0		127.2		127.5		126.8		127.5
2″	7.51 *d* (8.7)	131.1	7.49 *d* (8.5)	131.1	7.70 *d* (8.6)	133.9	7.47 *d* (8.5)	131.0	7.70 *d* (8.6)	133.8
3″	6.84 *d* (8.7)	116.7	6.82 *d* (8.5)	116.7	6.76 *d* (8.6)	115.8	6.81 *d* (8.5)	116.6	6.76 *d* (8.6)	115.7
4″		161.3		161.6		160.0		161.2		160.0
5″	6.84 *d* (8.7)	116.7	6.82 *d* (8.5)	116.7	6.76 *d* (8.6)	115.8	6.81 *d* (8.5)	116.6	6.76 *d* (8.6)	115.7
6″	7.51 *d* (8.7)	131.1	7.49 *d* (8.5)	131.1	7.70 *d* (8.6)	133.9	7.47 *d* (8.5)	131.0	7.70 *d* (8.6)	133.8
7″	7.70 *d* (15.9)	147.1	7.69 *d* (15.9)	147.2	6.92 *d* (12.7)	145.9	7.67 *d* (16.0)	147.2	6.92 *d* (12.6)	146.0
8″	6.40 *d* (15.9)	114.6	6.39 *d* (15.9)	114.6	5.83 *d* (12.7)	115.9	6.36 *d* (16.0)	114.4	5.82 *d* (12.6)	115.8
9″		168.4		168.5		167.2		168.2		166.9

Table 2
^{1}H NMR (700 MHz) and ^{13}C NMR data (175 MHz) of compounds **6**–**9** in MeOH-d_4.

Position	**6**		**7**		**8**		**9**	
	δ_H mult. (*J* in Hz)	δ_C	δ_H mult. (*J* in Hz)	δ_C	δ_H mult. (*J* in Hz)	δ_C	δ_H mult. (*J* in Hz)	δ_C
1		144.5		144.7		156.8		156.8
2		151.0		150.9		126.0		126.0
3	6.90 *dd* (8.2/1.4)	118.2	6.90 *dd* (1.3/8.1)	118.3	7.31 *d* (7.2)	130.6	7.31 *m*	130.6
4	7.03 *dd* (7.8/8.2)	126.7	7.03 *dd* (8.1/7.9)	126.8	7.04 *dd* (7.2/8.0)	123.5	7.04 *m*	123.5
5	6.80 *dd* (7.8/1.4)	120.9	6.81 *dd* (1.3/7.9)	121.0	7.33 *dd* (8.0/8.6)	131.0	7.33 *m*	131.0
6		131.2		131.2	7.24 *d* (8.6)	116.6	7.22 *d* (8.5)	116.6
7a	5.54 *d* (12.6)	64.7	5.53 *d* (12.6)	64.7	5.28 *d* (12.6)	64.3	5.28 *d* (12.3)	64.3
7b	5.30 *d* (12.6)		5.29 *d* (12.6)		5.40 *d* (12.6)		5.39 *d* (12.3)	
1′	4.72 *d* (8.2)	107.0	4.68 *d* (7.9)	106.9	5.01 *d* (7.8)	102.3	4.99 *d* (7.8)	102.3
2′	3.62 *dd* (8.2/9.0)	75.4	3.61 *dd* (7.9/8.8)	75.4	3.61 *dd* (7.8/9.5)	74.9	3.60 *m*	75.0
3′	3.74 *dd* (9.0/9.5)	75.6	3.69 *dd* (9.7/8.8)	75.4	3.78 *dd* (9.5/10.2)	75.6	3.71 *m*	76.0
4′	4.98 *dd* (9.5/9.0)	71.8	4.96 *dd* (9.7/9.7)	71.4	4.95 *dd* (9.2/10.2)	72.0	4.93 *dd* (9.3/9.8)	71.7
5′	3.57 *ddd* (1.8/6.6/9.0)	76.4	3.50 *ddd* (2.5/6.3/9.7)	76.3	3.70 *m*	76.3	3.64 *m*	76.1
6′a	3.57 *dd* (6.6/12.3)	62.0	3.63 *dd* (2.5/11.8)	62.0	3.58 *m*	62.1	3.64 *m*	62.0
6′b	3.64 *dd* (1.8/12.3)		3.57 *dd* (6.3/11.8)		3.65 *m*		3.57 *m*	
1″		126.9		127.5		126.9		127.4
2″	7.47 *d* (8.6)	131.1	7.68 *d* (8.5)	133.9	7.49 *d* (8.9)	131.1	7.69 d (8.5)	133.8
3″	6.81 *d* (8.6)	116.9	6.77 *d* (8.5)	115.7	6.82 *d* (8.9)	116.8	6.78 d (8.5)	115.7
4″		161.3		160.0		161.3		160.0
5″	6.81 *d* (8.6)	116.9	6.77 *d* (8.5)	115.7	6.82 *d* (8.9)	116.8	6.78 d (8.5)	115.7
6″	7.47 *d* (8.6)	131.1	7.68 *d* (8.5)	133.9	7.49 *d* (8.9)	131.1	7.69 d (8.5)	133.8
7″	7.67 *d* (15.9)	147.2	6.92 *d* (12.6)	146.1	7.69 *d* (15.6)	147.3	6.93 d (12.9)	146.0
8″	6.37 *d* (15.9)	114.5	5.81 *d* (12.6)	114.6	6.39 *d* (15.6)	114.6	5.83 d (12.9)	115.8
9″		168.4		167.2		168.5		167.2
1‴		79.1		79.3		79.1		79.1
2‴	5.75 *ddd* (9.8/1.5/1.5)	129.2	5.74 *ddd* (2.2/2.2/9.7)	129.0	5.77 *ddd* (1.8/1.9/9.7)	129.1	5.77 *m*	129.1
3‴	6.16 *ddd* (9.8/3.6/3.6)	133.0	6.16 *ddd* (3.9/3.9/9.7)	133.3	6.17 *m*	133.2	6.17 *m*	133.2
4‴a	2.64 *m*	27.0	2.64 *m*	27.0	2.52 *m*	27.1	2.52 *m*	26.5
4‴b	2.52 *m*		2.52 *m*		2.65 *m*		2.71 *m*	
5‴a	2.93 *m*	36.9	2.56 *m*	36.8	2.89 *m*	36.8	2.89 *m*	36.8
5‴b	2.57 *m*		2.92 *m*		2.54 *m*		2.54 *m*	
6‴		207.2		206.6		207.4		207.4
7‴		171.5		171.4		171.5		171.5

the presence of an (*E*)-*p*-coumaroyl moiety. The doublet signal of the proton at the anomeric position of a β-glycopyranosyl unit appeared at δ_H 4.38 ($^{3}J_{HH}$ = 7.8 Hz; H-1′) in the ^{1}H NMR spectrum. The corresponding ^{13}C chemical shift of C-1′ at δ_C 104.3 was extracted from the ^{1}H-^{13}C HSQC spectrum. Due to overlapping signals, selective total correlation spectroscopy (SELTOCSY)

experiments together with correlation data from ^{1}H-^{13}C HSQC and ^{1}H-^{1}H COSY were employed to extract the chemical shifts and positions of all members of the glycopyranosyl spin system (see Supplementary Data). The large values of the $^{3}J_{HH}$ coupling constants (Table 1) indicated axial configuration throughout the glucosyl ring, thus assigning the sugar unit as glucopyranose with β-configuration at position 1'. Remarkable low-field shifts for the signals of H-4'/C-4' (δ_H 4.85/δ_C 72.3) indicated substitution in this position. This assumption was further supported by the correlation of H-4′ to C-9″, which established an ester linkage of the (*E*)-*p*-coumaroyl unit to 4′-OH of the glucopyranosyl ring. A second SELTOCSY experiment was conducted to characterize a remaining AX_2A' spin system comprising two methylene units. Due to asymmetrical substitution, multiplet signals appeared at δ_H 3.69 and δ_H 3.98, with a corresponding ^{13}C chemical shift at δ_C 72.3 (C-1). An HMBC correlation showed this methylene group to be linked to position 1 of the β-glycosyl unit, C-1'. The multiplet signal of H-2/C-2 at δ_H 3.73/δ_C 62.2 indicated a hydroxylated terminus of the AX_2A' spin system. Accordingly, the structure of compound **1** was assigned as 1-*O*-(2-hydroxyethyl)-4-*O*-(*E*)-*p*-coumaroyl-β-glucopyranose.

The HRESIMS data of compound **2** showed a molecular ion peak of *m/z* 431.1336 [M-H]$^-$, which is consistent with a molecular formula of $C_{22}H_{24}O_9$ (calcd for $C_{22}H_{23}O_9$, *m/z* 431.1348). As for compound **1**, the ^{1}H NMR, ^{1}H-^{1}H COSY, ^{1}H-^{13}C HSQC and HMBC spectra showed signals of an (*E*)-*p*-coumaroyl unit connected to the 4′-OH position of a glycopyranosyl ring indicating a 4-(*E*)-*p*-coumaroyl-β-glucopyranose moiety (*E*-CG) (Table 1). Furthermore, the low-field range of the ^{1}H NMR spectrum showed a singlet at δ_H 7.13 (H-2), overlapping signals at δ_H 7.03 (H-6) and δ_H 7.02 (H-4) as well as a doublet of doublets at δ_H 7.27 (H-5) with coupling constants of $^{3}J_{HH}$ = 7.8/7.8 Hz. The corresponding ^{13}C chemical shifts were determined by ^{1}H-^{13}C HSQC to be δ_C 121.8 (C-4), δ_C 130.2 (C-5), δ_C 116.5 (C-6) and δ_C 116.1 (C-2), respectively. Due to ^{1}H-^{1}H COSY correlations, the signals of H-4, H-5 and H-6 were assigned to a three-spin system (AMX) of an aromatic ring. The $^{3}J_{CH}$ correlations of H-2, H-4 and H-6 in the ^{1}H-^{13}C HMBC spectrum corroborated the assignment of the corresponding carbon signals to a 1,3-disubstituted aromatic ring. The ring geometry was further characterized by long-range C-H correlations from H-5 to the signals of the quaternary carbon atoms at δ_C 159.2 (C-1) and δ_C 144.5 (C-3). HMBC correlations from H-4 and H-2 to C-7 (δ_C 64.8/δ_H 4.56) established the connection to a terminal hydroxymethylene unit tethered to C-3 of the aromatic ring. The low-field shift of C-1 (δ_C 159.2) indicated oxygenation at this position. This assumption was further supported by HMBC correlations of H-6 and H-2 to C-1' (δ_C 102.2), establishing the linkage via the ester bond to the anomeric carbon atom of the β-glycopyranosyl unit. Accordingly, the structure of compound **2** was assigned as 1-*O*-(3-hydroxymethylphenyl)-4-*O*-(*E*)-*p*-coumaroyl-β-glucopyranose.

Compound **3** showed a molecular ion peak of *m/z* 431.1337 [M-H]$^-$ in HRESIMS. As for compound **2**, its mass was consistent with a molecular formula of $C_{22}H_{24}O_9$ (calcd for $C_{22}H_{23}O_9$, *m/z* 431.1348), suggesting isomeric structures for compounds **2** and **3**. Furthermore, a comparison of ^{1}H NMR, ^{1}H-^{1}H COSY, ^{1}H-^{13}C HSQC and ^{1}H-^{13}C HMBC signals with those of **2** (Table 1) revealed a close structural similarity between the two compounds. NMR spectra indicated the presence of compound **2** in sample **3** which might be the result of a spontaneous isomerization. The only difference observed for **3** was a high-field shift of the π-system resonances of the *p*-coumaroyl moiety. The ^{1}H NMR spectrum showed doublet signals at δ_H 6.92 (H-7″) and δ_H 5.83 (H-8″), both with a coupling constant $^{3}J_{HH}$ = 12.7 Hz characteristic of the *Z*-configuration of a C-C double bond. Accordingly, the structure of compound **3** was determined to be 1-*O*-(3-hydroxymethylphenyl)-4-*O*-(*Z*)-*p*-coumaroyl-β-glucopyranose.

The HRESIMS data of compound **4** showed a molecular ion peak of *m/z* 447.1287 [M-H]$^-$ consistent with a molecular formula of $C_{22}H_{24}O_{10}$ (calcd for $C_{22}H_{23}O_{10}$, *m/z* 447.1297). The NMR spectra showed the same signals for the *E*-CG unit as spectra of compounds **1** and **2** did. Furthermore, the ^{1}H NMR data (Table 1) showed signals for a three-spin system (AMX) in the low-field region at δ_H 6.85 ($^{3}J_{HH}$ = 8.0 Hz, H-3), δ_H 7.03 ($^{3}J_{HH}$ = 8.0/7.5 Hz, H-4) and δ_H 6.89 ($^{3}J_{HH}$ = 7.5 Hz, H-5). The corresponding ^{13}C chemical shifts were determined by ^{1}H-^{13}C HSQC to be δ_C 117.2 (C-3), δ_C 126.7 (C-4) and δ_C 121.0 (C-5). The observed chemical shifts together with the $^{3}J_{HH}$ values suggested the presence of a 1,2,3-trisubstituted aromatic ring. This assumption was corroborated by the ^{1}H-^{13}C HMBC spectrum, which showed $^{3}J_{CH}$ correlations of H-3, H-5 and H-4 to a quaternary carbon atom at δ_C 144.3 (C-1). Additionally, H-4 showed strong $^{3}J_{CH}$ correlation to two other quaternary carbon atoms at δ_C 150.6 (C-2) and δ_C 136.5 (C-6), respectively, confirming the geometry of the aromatic ring. An HMBC correlation between H-5 and C-7 (δ_C 60.4) established the connection of the hydroxymethylene group to C-6 of the aromatic ring. Because of their large ^{13}C chemical shift values, the quaternary carbon atoms C-1 and C-2 of the ring were determined to be oxygenated. Furthermore, the characteristic high-field shift of C-1 indicated substitution in this position. This assumption was supported by a $^{3}J_{CH}$ correlation between the proton at the anomeric center of the *E*-CG glucose unit at δ_H 4.68 (H-1′) and C-1 in the ^{1}H-^{13}C HMBC spectrum. Accordingly, the structure of **4** was assigned as 1-*O*-(2-hydroxy-6-hydroxymethylphenyl)-4-*O*-(*E*)-*p*-coumaroyl-β-glucopyranose.

The HRESIMS data of compound **5** showed a molecular ion peak of *m/z* 417.1182 [M-H]$^-$ consistent with a molecular formula of $C_{21}H_{22}O_9$ (calcd for $C_{21}H_{21}O_9$, *m/z* 417.1191). The NMR spectra showed signals of the 4-(*Z*)-*p*-coumaroyl-β-glucopyranose moiety (*Z*-CG) resembling those observed earlier for compound **3**. Furthermore, the ^{1}H NMR spectrum showed signals (Table 1) assignable to protons of a four-spin system (ABCD) in the low-field region at δ_H 7.19 ($^{3}J_{HH}$ = 8.0/1.3 Hz, H-3), δ_H 6.78 ($^{3}J_{HH}$ = 8.0/7.6/1.5 Hz, H-4), δ_H 6.92 ($^{3}J_{HH}$ = 7.6/8.0/1.3 Hz, H-5) and δ_H 6.84 ($^{3}J_{HH}$ = 8.0/1.5 Hz, H-6), characteristic of a 1,2-disubstituted aromatic ring. The corresponding ^{13}C chemical shifts were extracted from ^{1}H-^{13}C HSQC data to be δ_C 117.0 (C-6), δ_C 124.8 (C-5), δ_C 120.8 (C-4) and δ_C 118.9 (C-3). The structure was further characterized by ^{1}H-^{13}C HMBC data, showing $^{3}J_{CH}$ correlations of H-4 with δ_C 146.3 (C-1) and H-5 with δ_C 147.7 (C-2). Because of their high ^{13}C chemical shift values, C-1 and C-2 were assumed to be oxygenated. Another HMBC correlation from the signal of H-1' (δ_H 4.81, $^{3}J_{HH}$ = 8.4) at the anomeric center to C-1 established the ester linkage of the aromatic ring to the β-glucopyranose of the *Z*-CG unit. Accordingly, the structure of compound **5** was assigned as 1-*O*-(2-hydroxyphenyl)-4-*O*-(*Z*)-*p*-coumaroyl-β-glucopyranose.

The HRESIMS data of compound **6** showed a molecular ion peak of *m/z* 585.1593 [M-H]$^-$ consistent with a molecular formula of $C_{29}H_{30}O_{13}$ (calcd for $C_{29}H_{29}O_{13}$, 585.1614). The NMR spectra showed signals similar to those observed for compound **4**. Additionally, the ^{1}H NMR spectrum (Table 2) showed two signals of a π-system at δ_H 5.75 ($^{3}J_{HH}$ = 9.8/1.5/1.5 Hz, H-2‴) and δ_H 6.16 ($^{3}J_{HH}$ = 9.8/3.6/3.6 Hz, H-3‴). The π-system was attached to two consecutive methylene groups at δ_H 2.64/2.52 (H-4‴a/b) and δ_H 2.93/2.57 (H-5‴a/b), as revealed by ^{1}H-^{1}H COSY cross-signals between H-3‴ and H-4‴. The corresponding ^{13}C chemical shifts were determined by ^{1}H-^{13}C HSQC to be δ_C 129.2 (C-2‴), δ_C 133.0 (C-3‴), δ_C 27.0 (C-4‴) and δ_C 36.9 (C-5‴). The ^{1}H-^{13}C HMBC spectrum showed a $^{3}J_{CH}$ correlation of H-2‴ with a quaternary carbon atom at δ_C 207.4 (C-6‴), which is characteristic of a keto functionality. Another HMBC correlation of H-3‴ with a second quaternary carbon atom at δ_C 79.1 (C-1‴) was observed, which was determined to

be oxygenated due to its ^{13}C chemical shift value. Further long-range CH-correlations suggested an aliphatic ring structure as corroborated by $^{3}J_{CH}$ correlations of H-5‴a/b to C-6‴ and H-5‴b to C-1‴. The geometry was also supported by $^{3}J_{CH}$ correlations of H-3‴/H-2‴ to C-4‴ and H-3‴ to C-5‴. An additional HMBC correlation of H-3‴ to a third quaternary carbon atom at δ_C 171.5 (C-7‴) indicated the linkage to a carboxyl functionality tethered to position C-1‴ of the aliphatic ring structure, which led to the characterization of the subunit as 1-hydroxy-cyclohex-2-en-6-onoyl moiety (HCH). Because another long-range CH-correlation from the methylene group of the aromatic ring at H-7a/b (δ_H 5.54/5.30; δ_C 64.7) to C-7‴ established the ester linkage of the HCH unit with the rest of the molecule, the structure was characterized as an idescarpin derivative (Fig. 1) with an additional *p*-coumaric acid linked to the 4′-OH of the *β*-glucopyranosyl moiety. Determination of the configuration at position C-1‴ in the HCH moiety was achieved by circular dichroism (CD) spectroscopy. The differential dichroic absorption of $\Delta\varepsilon = -6.9$ mdeg ($\lambda_{max} = 216$ nm, c = 0.75 mM, MeOH) of compound **6** was compared with the reported value of $\Delta\varepsilon = -13.4$ mdeg ($\lambda_{max} = 224$ nm, c = 1.61 mM) for (*S*)-idescarpin (Feistel et al., 2015; Kim et al., 2014). The negative $\Delta\varepsilon$ values reveal the same stereochemistry of **6** and idescarpin. Hence, we concluded that compound **6** had an (*S*)-configuration at the stereogenic position C-1‴. Accordingly, the structure of compound **6** was assigned as 4′-*O*-(*E*)-*p*-coumaroyl-idescarpin.

The HRESIMS data of compound **7** showed a molecular ion peak of *m/z* 585.1601 [M-H]$^-$. As for compound **6**, its mass was consistent with a molecular formula of $C_{29}H_{30}O_{13}$ (calcd for $C_{29}H_{29}O_{13}$, *m/z* 585.1614), suggesting isomeric structures for compounds **6** and **7**. Furthermore, a comparison of ^{1}H NMR, ^{1}H-^{1}H COSY, ^{1}H-^{13}C HSQC and ^{1}H-^{13}C HMBC data with those of compound **6** (Table 2) also suggested both compounds have very similar structures. Signals of compound **6** were also observed in the NMR spectra of compound **7**, which might be due to spontaneous isomerization. Compared to signals seen in the ^{1}H NMR spectrum of compound **6**, the proton signals of the *p*-coumaroyl π-system of compound **7** appeared at a higher field at δ_H 6.92 (H-7″) and δ_H 5.81 (H-8″). Both doublet signals showed a coupling constant of $^{3}J_{HH} = 12.6$ Hz, which indicates *Z*-configuration. CD spectroscopy resulted in $\Delta\varepsilon = -5.6$ mdeg ($\lambda_{max} = 218$ nm, c = 0.98 mM, MeOH), which is in accordance with the stereochemical description of compound **6** ((*S*)-configuration at position C-1‴). Accordingly, the structure of compound **7** was assigned as 4′-*O*-(*Z*)-*p*-coumaroyl-idescarpin.

Compounds **8** and **9** were obtained as a mixed fraction from HPLC-SPE-separation. UPLC-HRESIMS showed two molecular ions of *m/z* 569.1650 [M-H]$^-$ and *m/z* 569.1652 [M-H]$^-$, both corresponding to a molecular formula of $C_{29}H_{30}O_{12}$ (calcd for $C_{29}H_{29}O_{12}$, *m/z* 569.1664). The NMR data (Table 2) of compounds **8** and **9** showed close similarities with the data of compounds **6** and **7** described above. Matching signals for the presence of HCH rings as well as the *Z*-CG and *E*-CG moieties were found, indicating compounds **8** and **9** were a pair of *cis-trans* isomers. Comparative integration of the ^{1}H NMR signals of *E*-CG (**8**) (δ_H 6.39 with $^{3}J_{HH} = 15.6$, H-8″) and *Z*-CG (**9**) (δ_H 5.83 with $^{3}J_{HH} = 12.9$, H-8″) revealed a molar ratio of 2 to 1. Structure elucidation of compound **8** started from the NMR signals of its *E*-CG unit. The ^{1}H NMR signal of the proton (H-1′) at the anomeric position of a *β*-glucopyranosyl unit appeared at δ_H 5.01 ($^{3}J_{HH} = 7.8$ Hz). This signal showed a ^{1}H-^{13}C HMBC correlation to a quaternary carbon atom at δ_C 156.8. The chemical shift assigned the latter signal to the oxygenated C-1 of an aromatic system. The aromatic proton signals were assigned to a four-spin system (ABCD) consisting of δ_H 7.31 ($^{3}J_{HH} = 7.2$ Hz, H-3), δ_H 7.04 ($^{3}J_{HH} = 7.2/8.0$ Hz, H-4), δ_H 7.33 ($^{3}J_{HH} = 8.0/8.6$ Hz, H-5) and δ_H 7.24 ($^{3}J_{HH} = 8.6$ Hz, H-6). The corresponding ^{13}C chemical shifts were determined from ^{1}H-^{13}C HSQC correlations to be δ_C 130.6 (C-3), δ_C 123.5 (C-4), δ_C 131.0 (C-5) and δ_C 116.6 (C-6). The 1,2-disubstitution was determined from characteristic HMBC correlations of H-6 and H-4 with a quaternary carbon atom at δ_C 126.0 (C-2) and of H-3 and H-5 with C-1. The HMBC correlation between the protons H-7a/b at δ_H 5.28/5.40 ($^{3}J_{HH} = 12.6$) of the hydroxymethylene group to C-3 (δ_C 130.6) indicated that this substituent is attached to C-2 of the aromatic ring. Thus, the fragment was characterized as a salicylic alcohol moiety. Further $^{3}J_{CH}$ correlations between position H-7a/b and the carboxyl carbon atom C-7‴ (δ_C 171.5) revealed the linkage to the HCH moiety via an ester bond. Accordingly, the structure of compound **8** was assigned as 4′-*O*-(*E*)-*p*-coumaroyl-salicortin. Except for the signals of its CG unit, compound **9** showed very similar chemical shift values compared to **8** (Table 2). Although most signals were overlapping, the connectivities of the particular subsystems appeared to be identical. Accordingly, the structure of compound **9** was assigned as 4′-*O*-(*Z*)-*p*-coumaroyl-salicortin.

As for compounds **6** and **7**, the configuration at the stereogenic position C-1‴ in the HCH moieties of **8** and **9** was determined by CD spectroscopy. A differential dichroic absorption of $\Delta\varepsilon = -3.5$ mdeg ($\lambda_{max} = 219$ nm, c = 1.19 mM, MeOH) was found for the mixture and compared with the reported value of $\Delta\varepsilon = -26.7$ mdeg ($\lambda_{max} = 224$ nm, c = 1.61 mM) for salicortin (Fig. 1) (Feistel et al., 2015). Accordingly, (*S*)-configuration at position C-1‴ was concluded. Usually, determination of the configuration demands pure substances. However, here we determined $\Delta\varepsilon$ for a mixture of the isomeric compounds **8** and **9**; these differ only in the configuration of their double bond system, which does not interfere with the stereogenic position of interest. The very similar NMR spectra of these compounds highlight their close electronic similarity. However, in contrast to the reference compound salicortin, compounds **8** and **9** have stronger UV absorption due to the presence of additional chromophores, and these in turn influence the CD measurement. As a result, the determined $\Delta\varepsilon$ is still negative, but smaller compared to $\Delta\varepsilon$ of salicortin. Furthermore, the (*S*)-configuration of the main HCH-containing compounds idescarpaside (**14**) and idescarpin (**15**) was determined earlier by X-ray crystallography (Kim et al., 2014).

The HRESIMS of compound **12** showed a molecular ion peak of *m/z* 423.1651 [M-H]$^-$, which corresponds to a molecular formula of $C_{21}H_{28}O_9$ (calcd for $C_{21}H_{27}O_9$, *m/z* 423.1661). According to reported data (Si et al., 2009), the observed NMR signals suggest that this compound is an isograndidentatin isomer. The 1,2-cyclohexanediol ring of this structure features two stereogenic centers at positions C-1 and C-2. NMR data were inconsistent with (1*R*,2*S*)-*cis*-configuration (Si et al., 2009) and (1*S*,2*S*)-*trans*-configuration (Pichette et al., 2010). To the best of our knowledge (SciFinder® search, May 2017), no information about a possible (1*R*,2*R*)-*trans*-configured 1,2-cyclohexanediol has been reported. Therefore, compound **12** was hydrolyzed and the resulting aglycon was compared to authentic standards by chiral GC-MS measurements. The hydrolysis product was determined to be (1*R*,2*S*)-*cis*-1,2-cyclohexanediol. Accordingly, we identified **12** as isograndidentatin A.

The structures of compounds **1**–**15** from *I. polycarpa* resemble those of compounds reported from *Salix* (Thieme, 1964) and *Populus* species (Boeckler et al., 2011; Dommisse et al., 1986; Si et al., 2009). However, a typical *Idesia* feature is the presence of compounds with an additional hydroxyl group in the aromatic part of the parent salicinoids (**4**, **6**, **7** and **14**, **15**). Whereas *β*-glucopyranose substituents in compounds isolated from *Populus* are typically found on position C-2′ or C-6′, the corresponding *Idesia* compounds are acylated exclusively at position C-4' (**1**–**9** and **11**–**13**).

Little is known about the ecological functions of *Idesia* constituents. Like *Populus* salicinoids, which are generally accepted as defense compounds with feeding-deterrent and anti-fungal

activity (Julkunen-Tiitto et al., 1994; Massad et al., 2014; Yang et al., 2013), the isolated compounds might also play a role in chemical defense. The HCH subunit, part of *Idesia* salicinoids (**6**–**9**, **14**, **15**), is believed to be oxidatively converted after hydrolysis, leading to *o*-quinones (Clausen et al., 1989; Haruta et al., 2001). The *o*-quinones may function as cross-linkers of dietary or digestive proteins in herbivores (Clausen et al., 1989; Haruta et al., 2001; Ruuhola et al., 2003). Furthermore, *p*-coumaroyl units in *Idesia* constituents may serve as substrates for an oxidative transformation, yielding further *o*-quinone derivatives (Chang, 2009), and these may increase feeding-deterrent activity.

2.2. Performance of lepidopteran larvae

2.2.1. Using C. vinula and L. dispar to determine anti-herbivory properties of leaf constituents

Feeding experiments were conducted to address the questions of whether and to what extent *Idesia* leaf constituents have anti-herbivory properties. Larvae of two insect species, *C. vinula,* a specialist herbivore whose life cycle is adapted to plants of the Salicaceae, and the generalist herbivore *L. dispar,* which has a broad range of host plants, were used in this study. Both species are able to thrive on nutrient sources containing salicinoids. The test insects were reared on *P. nigra* prior to the feeding assays and *P. nigra* diet served as a control in the experiments. To determine herbivore performance, 3rd-instar larvae of both species were placed in arenas equipped with leaves of *I. polycarpa*. The control group was supplied with *P. nigra* leaves. Performance of larvae was monitored as average mass for six days by daily balancing each individual. Due to mortality of some larvae, a statistical time frame from day 0 to day 4 was used. Furthermore, leaf consumption was determined as total consumed leaf area a_{total} as described in Experimental.

2.2.2. Performance of specialist herbivore C. vinula

The mass of *C. vinula* depended on the time (likelihood ratio = 24.378, $p < 0.001$) and the plant the larvae fed on (likelihood ratio = 42.285, $p < 0.001$). Whether *C. vinula* larvae gained mass over time, however, depended on the plant they fed on (interaction time: plant: likelihood ratio 172.041, $p < 0.001$). Only larvae fed on *P. nigra* gained mass (Fig. 2A). The average mass of *C. vinula* larvae fed on *I. polycarpa* leaves decreased from 81 mg on day 0 to 68 mg on day 4, corresponding to an average mass loss of 2 mg per day. High mortality was observed, with 50% of individuals dead after four days. None of the larvae survived day 5 (Fig. 2B). All larvae changed their color from green to a dark yellowish shade. Additionally, fecal consistency changed from solid pellets to liquid excretions. Both symptoms might be interpreted as an effect of starvation caused by deterrent leaf ingredients. The control group fed on *P. nigra* leaves showed a strong increase of average mass from 97 mg (day 0) up to 697 mg (day 5), corresponding to a mass gain of 100 mg per day. The fold mass gain was dependent on the leaf area the larvae consumed during the experiment ($F = 689.086$ $p < 0.001$). When fed on *P. nigra* they gained significantly more mass compared to the *I. polycarpa* ($F = 48.620$ $p < 0.001$) diet. However, how much mass the caterpillars gained per ingested leaf area was different for the two plants ($F = 4.807$ $p = 0.049$). Caterpillars that fed on *P. nigra* gained mass but caterpillars fed on *I. polycarpa* slightly lost mass (Fig. 3A). These observations clearly show that *I. polycarpa* was highly toxic to *C. vinula* larvae.

2.2.3. Performance of generalist herbivore L. dispar

Larvae of L. *dispar* fed on *P. nigra* gained ca. 27 mg mass per day with an increase from 187 mg on day 0 to 301 mg on day 3. Larvae did not continue to grow after day 3. *L. dispar* fed on *I. polycarpa* grew slowly (187 mg on day 0 to 206 mg on day 5) (Fig. 2C). The mass of *L. dispar* also depended on the time (likelihood ratio = 23.374, $p < 0.001$). Compared to *C. vinula* (Fig. 2A), the change in mass over the experimental time was less prominent. Statistically, it did not change according to the plant the larvae fed on (likelihood ratio = 0.643, $p = 0.423$). However, whether *L. dispar* larvae gained mass over time did depend on the plant species they fed on (interaction time: plant: likelihood ratio 13.888, $p = 0.008$). Only when fed on *P. nigra* the larvae gained mass. By day 5 the majority (70%) of *L. dispar* larvae fed on *I. polycarpa* were deceased (Fig. 2D). The fold mass gain was only dependent on the amount the larvae fed during the experiment ($F = 18.107$ $p = 0.001$), but not on the plant species they fed on ($F = 0.196$ $p = 0.666$). How much mass the caterpillars gained per consumed leaf area was same for both plants ($F = 0.355$ $p = 0.563$) (Fig. 3B).

2.2.4. Survivorship of C. vinula and L. dispar

Both Lepidopteran species survived significantly better on *P. nigra* than on *I. polycarpa* ($z = -3.592$, $p < 0.001$). The survival rate of both species of larvae was the same ($z = -1.161$, $p = 0.2458$), and they reacted the same way to both plant species (interaction between plant and herbivore $z = 0.998$, $p = 0.318$) (Fig. 2).

3. Conclusions

In this work, 15 compounds from leaves of *I. polycarpa* were isolated and identified by means of spectroscopic methods. Compounds **1**–**9** are described for the first time as natural products. Compounds **1**–**13** had not previously been reported as constituents of *I. polycarpa*. These compounds are structurally related to salicinoids, which are known defense compounds from *Salix* and *Populus* species. Feeding experiments with larvae of the Salicaceae specialist herbivore *C. vinula* and the broadleaf tree generalist *L. dispar* showed differences in performance. Both insect species performed worse on *I. polycarpa* than on *P. nigra*. Although *C. vinula* larvae performed much better on *P. nigra* than the generalist *L. dispar*, total mortality on *I. polycarpa* was observed after five days. We observed a higher survivorship for *L. dispar* on *I. polycarpa* (30% in total) but with less leaf area consumed and less mass gain in comparison to larvae fed with *P. nigra*. In order to interpret the results, the adaption strategies of the insect larvae has to be taken into account. To compete effectively, specialists are extremely adapted to their ecosystems and hence much more dependent on the environmental conditions (Ali and Agrawal, 2012). As a result, a slight change in nutrition, for example, might have a notable impact on their fitness. The performance of generalists is more robust, as our observations indicate. It can be hypothesized that the differential toxicity is caused by different mechanisms of detoxification (Boeckler et al., 2016) or that plant defensive proteins such as protease inhibitors (Neiman et al., 2009) or polyphenol oxidases (Wang and Constabel, 2004) interfere with digestion by decreasing nutrient availability. Another reason for the mortality observed may be compounds unnoticed by UV/Vis detection. The combined effect of those compounds may interfere with digestion and eventually negatively affect nutrient acceptance; in our experiments, this may have resulted finally in the starvation of the tested lepidopteran larvae.

4. Experimental

4.1. General experimental procedures

Solvents used for extraction and chromatographic separation were purchased from Carl Roth GmbH, Karlsruhe, Germany, and VWR International GmbH, Darmstadt, Germany, and were used without further purification. The synthetic reference compounds

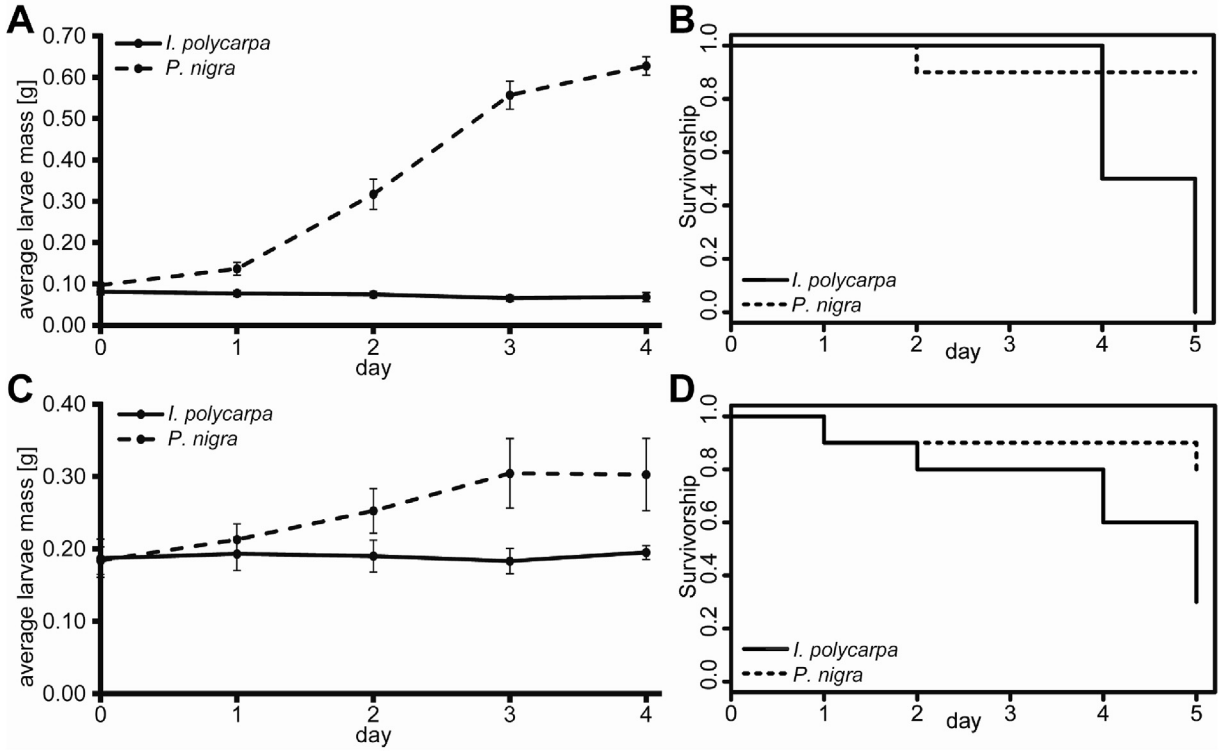

Fig. 2. Performance of lepidopteran larvae fed on *P. nigra* (dashed lines) and *I. polycarpa* (filled lines). Error bars represent standard errors. (**A**) Average mass of 3rd-instar larvae of *C. vinula*. (**B**) Kaplan-Meier graph illustrating the survivorship of *C. vinula*. (**C**) Average mass of 3rd-instar larvae of *L. dispar*. (**D**) Kaplan-Meier graph illustrating the survivorship of *L. dispar* larvae. (**A**) and (**C**) show the statistically analyzed time frame (day 0–4).

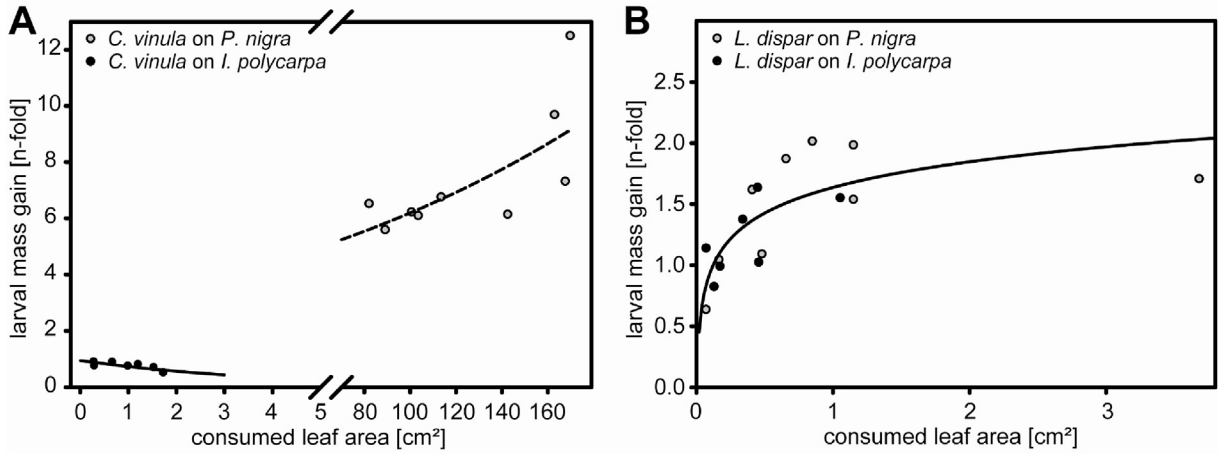

Fig. 3. Larval mass gain of *C. vinula* (**A**) and *L. dispar* (**B**) fed on *P. nigra* (black dots) and *I. polycarpa* (grey dots) including trend lines. Data were collected during 6 days for both experiments.

(1*R*,2*S*)-*cis*-cyclohexane diol, (1*S*,2*S*)-*trans*-cyclohexane diol and (1*R*,2*R*)-*trans*-1,2-cyclohexanediol were purchased from Sigma-Aldrich Chemie GmbH, Taufkirchen, Germany. Water used for HPLC was obtained from a Milli-Q Synthesis A 10 purifier (Merck KGaA, Darmstadt, Germany). Phytacon vessels (H 140 mm, base diam. 86 mm) used as arenas for the feeding experiments were purchased from Sigma-Aldrich. HR-X SPE cartridges (500 mg sorbent/6 ml volume) were purchased from Macherey-Nagel, Düren, Germany.

HPLC separations were carried out on an Agilent 1100 HPLC system, consisting of a degasser, quaternary solvent delivery pump G1311A, an autosampler G1313A (Agilent Technologies GmbH, Waldbronn, Germany) and a photodiode array detector (detection 200–700 nm; J&M Analytik AG, Aalen, Germany). An Isis RP-18e column (250 × 4.6 mm, 5 μm particle size) (Macherey-Nagel) was used for all separations. Column temperature was set to 30 °C, and the solvent flow rate was 0.8 ml min^{-1} using 0.1% formic acid in water and 0.1% formic acid in MeOH as a binary solvent system. An HPLC gradient starting with a 5 min isocratic flow of 30% MeOH and then linearly increasing for 90 min to 50% MeOH was used. After each run, the column was washed with 100% MeOH for 10 min and equilibrated with 30% MeOH for 10 min. The column outlet was connected to a Bruker/Spark Prospect 2 solid-phase extraction (SPE) system (Bruker Biospin GmbH, Rheinstetten, Germany),

equipped with HySphere GP resin cartridges. To reduce the eluotropic capacity of the HPLC solvent mixture, water with a flow rate of 2.5 ml min^{-1} was added using a make-up pump (Knauer, Berlin, Germany). SPE cartridges loaded with metabolites were dried in a stream of nitrogen prior to elution with MeOH. Eluted compounds were dried using a Genevac HT-4X vacuum centrifuge (Genevac Ltd., Ipswich, UK).

The hydrolysis products of compound **12** as well as the isomeric cyclohexane diol references were analyzed using an Agilent 7890A gas chromatograph equipped with a chiral Cyclosil-B column (30 m × 0.25 mm ID with 0.25 μm film thickness, Agilent) coupled to a quadrupole mass spectrometer Agilent 5975C. The carrier gas was helium at a constant flow of 2 ml min^{-1}. One microliter of each sample was injected in splitless mode. The inlet temperature was set to 230 °C. The oven program started at 40 °C for 5 min, increased at 1 °C min^{-1} to 90 °C, held for 10 min, then increased at 0.1 °C min^{-1} to 95 °C, and finally at 30 °C min^{-1} to 230 °C. MS conditions were electron impact mode (70 eV), and scan mode 33–250 amu.

ESI-HRMS data were measured in negative and positive mode at a mass resolution of $m/\Delta m$ 30.000 on a UHPLC system Ultimate 3000 series RSLC (Dionex) combined with LTQ Orbitrap XL mass spectrometer (Thermo Fisher Scientific, Bremen, Germany). Separation was done on an Acclaim C18 column (150 × 2.1 mm, 2.2 μm; Dionex, Sunnyvale, CA, USA) with a flow rate of 300 μL min^{-1} using the following gradient conditions: MeCN in water, both containing 0.1% (v/v) formic acid: constant at 1% for 8 min, linearly increased to 85% within 7 min, kept constant at 85% for 4 min, finally returning to 1% for equilibration for 4 min.

NMR spectra (^{1}H NMR, 1D NOESY, ^{1}H-^{1}H COSY, SELTOCSY, HMBC, HSQC) were recorded on a Bruker Avance III HD 700 spectrometer, equipped with a cryoplatform and a 1.7 mm TCI microcryoprobe (Bruker Biospin GmbH, Rheinstetten, Germany). NMR tubes of 1.7 mm outer diameter were used for all measurements. All NMR spectra were recorded using MeOH-d_4 as a solvent. Chemical shifts were referenced to the residual solvent peaks at δ_H 3.31 and δ_C 49.15, respectively. Data acquisition and processing were accomplished using TopSpin 3.2. (Bruker Biospin). Standard pulse programs as implemented in TopSpin were used for data acquisition.

CD spectra were recorded on a Jasco J-810 CD spectropolarimeter (Jasco GmbH, Gross-Umstadt, Germany). Compounds were measured in MeOH using a quartz cuvette of 1 mm width. Spectra were recorded for 185–350 nm and were accumulated 10 times. Baseline correction was performed on the basis of a MeOH blank sample.

4.2. Plant material and insect larvae

I. polycarpa trees were purchased in 2015 from Baumschule Pflanzenvielfalt GmbH, Zetel, Germany, and maintained in the Max Planck Institute of Chemical Ecology (MPI-CE) Jena, Germany. Leaf samples of black poplar (*P. nigra*) were taken from trees growing in the area surrounding the Max Planck Institute of Chemical Ecology (MPI-CE) Jena, Germany. *C. vinula* (Lepidoptera) larvae were taken from a colony reared at the MPI-CE, hatched from eggs and maintained on *P. nigra* until they reached the 3rd instar. *L. dispar* (gypsy moth) (Lepidoptera) larvae (3rd instar), reared on a *P. nigra* leaf diet, were kindly provided by Dr. Sybille Unsicker, MPI-CE.

4.3. Extraction and isolation

The leaves of *I. polycarpa* were lyophilized, resulting in 4.8 g of dried material; this was ground in a ceramic mortar and extracted (7 × 60 ml, each 15 min) with MeCN. The combined extracts were filtered and evaporated using a rotary evaporator, resulting in 598 mg crude extract (8% of the dried leaf material). The extract was reconstituted with 30 ml water and centrifuged to separate insoluble matter. The supernatant was subjected to pre-separation on a HR-X SPE cartridge. After conditioning with MeOH (2 × 6 ml) and equilibration with water (3 × 6 ml), the cartridge was loaded and washed with water (3 × 6 ml). After air-drying, the cartridge was eluted with MeOH (3 × 6 ml) and the combined fractions were evaporated in a vacuum centrifuge, resulting in 259 mg methanolic crude extract. For separation, an aliquot of the crude extract was reconstituted with MeOH (78.6 mg ml^{-1}) and subjected to HPLC-SPE to yield the following compounds (R_t retention time): **1** (R_t 9.18 min, 0.10% of leaf d.w.), **10** (R_t 14.43 min, 0.09%), **15** (R_t 21.16 min, 1.10%), **2** (R_t 27.18 min, 0.13%), **3** (R_t 30.73 min, 0.11%), **11** (R_t 36.47 min, 0.08%), **4** (R_t 42.92 min, 0.10%), **12** (R_t 45.55 min, 0.10%), **13** (R_t 52.16 min, 0.20%), **5** (R_t 55.55 min, 0.11%), **14** (R_t 58.84 min, 0.16%), **8** & **9** (R_t 70.84 min, 0.19%), **6** (R_t 77.58 min, 0.09%), **7** (R_t 79.58 min, 0.08%).

4.4. Hydrolysis of isograndidentatin A (*12*)

In order to determine the absolute configuration of compound **12**, acidic hydrolysis was carried out. Compound **12** (125 μg; 0.3 μmol) was dissolved in 500 μL MeOH and added to a stirred solution of 4.5 ml MeOH:H_2O (1:1, v/v) containing 150 μL of conc. HCl. The mixture was refluxed for 8 h, and then dried in a stream of nitrogen gas. The residue was dissolved in CH_2Cl_2 and analyzed by gas chromatography – mass spectrometry (GC-MS) together with the reference standards (1*R*,2*S*)-*cis*-cyclohexane diol, (1*S*,2*S*)-*trans*-cyclohexane diol and (1*R*,2*R*)-*trans*-1,2-cyclohexanediol. Based on retention time and mass spectrum, the absolute configuration was determined.

4.5. Performance of C. vinula and L. dispar on I. polycarpa

For feeding experiments, 10 × 1 *I. polycarpa* leaves and, as a control, 10 × 1 *P. nigra* leaves with a leaf plastochron index (LPI) from 3 to 10, were placed in 20 separate arenas with their petioles immersed in a 25 ml glass beaker filled with cotton wetted with tap water. One *C. vinula* larva was placed on each leaf. Thus, ten feeding experiments per plant species were conducted in parallel. During the experiment, the mass of each larva was determined every day. Leaves were replaced when consumed or exchanged every second day. In order to detect consumption, leaves were scanned and printed in 1:1 scale on paper (80 g m^{-2}). After feeding, the consumed leaf area was reconstructed by comparison with the reference scans, cut out and weighed (m_{paper} *in mg*). The total consumed leaf area a_{total} was calculated according to Eqn. (1). The feeding experiment with *L. dispar* larvae was performed accordingly.

$$a_{total} = \frac{m_{paper}}{8}\mathrm{cm}^2 \quad (1)$$

4.6. Statistical analysis

Because just a few larvae survived until day 5, larval masses were only analyzed until day 4 in order to have a sufficient number of replicates and because the two herbivore species generally differ in size, the change in their mass over time was analyzed separately. In order to test whether the caterpillars differed in their mass development depending on the plant they were feeding on, linear mixed effects models were applied (lme, nlme library (Pinheiro et al., 2016)) with plant and time as fixed factors and the larvae identity as a random intercept. In order to achieve normality of

residuals, data were log-transformed. For mass data from *C. vinula*, the varIdent variance structure (to allow data from each plant species to have a different variance) was applied to achieve variance homogeneity. P values were obtained by a stepwise removal of the explanatory variables and comparison of the more complex model with the simpler model with a likelihood ratio test (Zuur et al., 2009). The Cox proportional hazard model (coxph of the survival library (Therneau, 2015)) was used to investigate the survival of *C. vinula* and *L. dispar* on *P. nigra* and *I. polycarpa*. The model was simplified by removing non-significant factors. All analyses were done in R 3.3.1 (R Core Team, 2016).

In order to see to which extent larval mass was depending on the consumed leaf area *C. vinula* and *L. dispar* larvae were separately fed with either *P. nigra* or *I. polycarpa* leaves for 6 days. Data from non-feeding larvae were discarded from the analysis. For all other larvae it was considered how much they changed mass with respect to their start mass; the ratio of end mass and start mass gave an *n*-fold increase of mass for the respective larva. An analysis of covariance (ancova) with the consumed leaf area as continuous variable and the different food plants as categorical explanatory variable was undertaken. For the data analysis of *C. vinula* larvae mass gain data were log-transformed and for *L. dispar* larvae the consumed leaf area data were log-transformed to achieve homogeneity of variances and normality of the residuals.

4.7. Spectroscopic data of new compounds

4.7.1. 1-O-(2-Hydroxyethyl)-4-O-(E)-p-coumaroyl-β-glucopyranose (**1**)

UV (MeOH/H_2O): λ_{max} = 228, 313 nm; HRESIMS: *m/z* 369.1185 $[M-H]^-$ (calcd for $C_{17}H_{21}O_9$, 369.1191); ^1H and ^{13}C NMR, see Table 1.

4.7.2. 1-O-(3-Hydroxymethylphenyl)-4-O-(E)-p-coumaroyl-β-glucopyranose (**2**)

UV (MeOH/H_2O): λ_{max} = 210, 313 nm; HRESIMS: *m/z* 431.1336 $[M-H]^-$ (calcd for $C_{22}H_{23}O_9$, 431.1348); ^1H and ^{13}C NMR, see Table 1.

4.7.3. 1-O-(3-Hydroxymethylphenyl)-4-O-(Z)-p-coumaroyl-β-glucopyranose (**3**)

UV (MeOH/H_2O): λ_{max} = 209, 313 nm; HRESIMS: *m/z* 431.1337 $[M-H]^-$ (calcd for $C_{22}H_{23}O_9$, 431.1348); ^1H and ^{13}C NMR, see Table 1.

4.7.4. 1-O-(6-Hydroxy-2-hydroxymethylphenyl)-4-O-(E)-p-coumaroyl-β-glucopyranose (**4**)

UV (MeOH/H_2O): λ_{max} = 272, 316 nm; HRESIMS: *m/z* 447.1287 $[M-H]^-$ (calcd for $C_{22}H_{23}O_{10}$, 447.1297); ^1H and ^{13}C NMR, see Table 1.

4.7.5. 1-O-(2-Hydroxyphenyl)-4-O-(Z)-p-coumaroyl-β-glucopyranose (**5**)

UV (MeOH/H_2O): λ_{max} = 212, 281, 309 nm; HRESIMS: *m/z* 417.1182 $[M-H]^-$(calcd for $C_{21}H_{21}O_9$, 417.1191); ^1H and ^{13}C NMR, see Table 1.

4.7.6. 4′-O-(E)-p-Coumaroyl-idescarpin (**6**)

UV (MeOH/H_2O): λ_{max} = 216, 312 nm; CD: $\Delta\varepsilon$ = −6.9 mdeg (λ_{max} = 216 nm, c = 0.75 mM, MeOH); HRESIMS: *m/z* 585.1593 $[M-H]^-$ (calcd for $C_{29}H_{29}O_{13}$, 585.1614); ^1H and ^{13}C NMR, see Table 2.

4.7.7. 4′-O-(Z)-p-Coumaroyl-idescarpin (**7**)

UV (MeOH/H_2O): λ_{max} = 218, 310 nm; CD: $\Delta\varepsilon$ = −5.6 mdeg (λ_{max} = 218 nm, c = 0.98 mM, MeOH); HRESIMS: *m/z* 585.1601 $[M-H]^-$ (calcd for 585.1614, $C_{29}H_{29}O_{13}$); ^1H and ^{13}C NMR, see Table 2.

4.7.8. 4′-O-(E)-p-Coumaroyl-salicortin (**8**)

UV (MeOH/H_2O): λ_{max} = 210, 313 nm; CD: $\Delta\varepsilon$ = −3.5 mdeg (λ_{max} = 219 nm, c = 1.19 mM, MeOH); HRESIMS: *m/z* 569.1650 $[M-H]^-$ (calcd for 569.1664, $C_{29}H_{29}O_{12}$); ^1H and ^{13}C NMR, see Table 2.

4.7.9. 4′-O-(Z)-p-Coumaroyl-salicortin (**9**)

UV (MeOH/H_2O): λ_{max} = 210 nm, 313 nm; $\Delta\varepsilon$ = −3.5 mdeg (λ_{max} = 219 nm, c = 1.19 mM, MeOH); HRESIMS: *m/z* 569.1652 $[M-H]^-$ (calcd for 569.1664, $C_{29}H_{29}O_{12}$); ^1H and ^{13}C NMR, see Table 2.

4.8. Spectroscopic data of known compounds

Icaraside B2 (**10**): UV (MeOH/H_2O): λ_{max} = 230, 310 nm; HRESIMS: *m/z* 409.1831 $[M+Na]^+$ (calcd for $C_{19}H_{30}O_8Na$, 409.1833); ^1H and ^{13}C NMR, see S10.1 (Lee, 2012; Otsuka et al., 1995).

4-(*E*)-*p*-Coumaroyl-D-glucopyranose (**11**): UV (MeOH/H_2O): λ_{max} = 212, 313 nm; HRESIMS: *m/z* 349.0890 $[M+Na]^+$ (calcd for $C_{15}H_{18}O_8Na$), 349.0894; ^1H and ^{13}C NMR, see S10.9 (Birkofer et al., 1969; She et al., 2008).

Isograndidentatin A (**12**): UV (MeOH/H_2O): λ_{max} = 210, 222, 313 nm; HRESIMS: *m/z* 423.1651 $[M-H]^-$ (calcd for $C_{21}H_{27}O_9$, 423.1661); ^1H and ^{13}C NMR, see S11.12 (Si et al., 2009).

1-*O*-(2-Hydroxyphenyl)-4-*O*-(*E*)-p-coumaroyl-β-D-glucopyranose (**13**): UV (MeOH/H_2O): λ_{max} = 212, 313 nm; HRESIMS: *m/z* 417.1182 $[M-H]^-$ (calcd for $C_{21}H_{21}O_9$, 417.1191); ^1H and ^{13}C NMR, see S12.3 (Kumar et al., 2010).

Idescarparide (**14**): UV (MeOH/H_2O): λ_{max} = 215, 275 nm; CD: $\Delta\varepsilon$ = −11.5 mdeg (λ_{max} = 215 nm, c = 0.55 mM, MeOH); HRESIMS: *m/z* 903.2532 $[M+Na]^+$ (calcd for $C_{40}H_{48}O_{22}Na$, 903.2529); ^1H and ^{13}C NMR, see S13.3 (Kim et al., 2014).

Idescarpin (**15**): UV (MeOH/H_2O): λ_{max} = 215, 277, 311 nm; CD: $\Delta\varepsilon$ = −11.5 mdeg (λ_{max} = 215 nm, c = 0.55 mM, MeOH); HRESIMS: *m/z* 463.1200 $[M+Na]^+$ (calcd for $C_{20}H_{24}O_{11}Na$, 463.1211); ^1H and ^{13}C NMR, see S14.1 (Feistel et al., 2015).

Acknowledgments

The authors thank Dr. Sybille Unsicker for providing *L. dispar* larvae, Regina Seibt for her support in rearing *C. vinula*, and Emily Wheeler for editorial assistance.

Appendix A. Supplementary data

Supplementary data related to this article can be found at http://dx.doi.org/10.1016/j.phytochem.2017.08.008.

References

Ali, J.G., Agrawal, A.A., 2012. Specialist versus generalist insect herbivores and plant defense. Trends Plant Sci. 17, 293–302.
Baek, S., Kim, D., Lee, C., Kho, Y., Lee, C., 2006. Idescarpin isolated from the fruits of *Idesia polycarpa* inhibits melanin biosynthesis. J. Microbiol. Biotechnol. 16, 667–672.
Birkofer, L., Kaiser, C., Hillges, B., Becker, F., 1969. NMR-spektroskopische Untersuchungen von Acyl-glykosen. Justus Liebigs Ann. Chem. 725, 196–202.
Boeckler, G.A., Gershenzon, J., Unsicker, S.B., 2011. Phenolic glycosides of the Salicaceae and their role as anti-herbivore defenses. Phytochemistry 72, 1497–1509.
Boeckler, G.A., Paetz, C., Feibicke, P., Gershenzon, J., Unsicker, S.B., 2016. Metabolism of poplar salicinoids by the generalist herbivore *Lymantria dispar* (Lepidoptera). Insect Biochem. Mol. Biol. 78, 39–49.
Chang, T.-S., 2009. An updated review of tyrosinase inhibitors. Int. J. Mol. Sci. 10, 2440–2475.
Chou, C.-J., Lin, L.-C., Tsai, W.-J., Hsu, S.-Y., Ho, L.-K., 1997. Phenyl-β-D-glucopyranoside derivatives from the fruits of *Idesia polycarpa*. J. Nat. Prod. 60, 375–377.
Clausen, T.P., Reichardt, P.B., Bryant, J.P., Werner, R.A., Post, K., Frisby, K., 1989. Chemical model for short-term induction in quaking aspen (*Populus tremuloides*) foliage against herbivores. J. Chem. Ecol. 15, 2335–2346.
Dommisse, R.A., Van Hoof, L., Vlietinck, A.J., 1986. Structural analysis of phenolic glucosides from Salicaceae by NMR spectroscopy. Phytochemistry 25, 1201–1204.
Feistel, F., Paetz, C., Lorenz, S., Schneider, B., 2015. The absolute configuration of

salicortin, HCH-salicortin and tremulacin from *Populus trichocarpa* x *deltoides* Beaupré. Molecules 20, 5566–5573.
Guo, H., Shen, Q.-W., Hu, Y.-C., 2012. Quality analysis of *Idesia polycarpa* maxim seed oil. Xiandai Shipin Keji 28, 345–347.
Haruta, M., Pedersen, J.A., Constabel, C.P., 2001. Polyphenol oxidase and herbivore defense in trembling aspen (*Populus tremuloides*): cDNA cloning, expression, and potential substrates. Physiol. Plant 112, 552–558.
Hintze-Podufal, C., 1970. Über die quantitativen Änderungen der Kotabgabe während der Larvalentwicklung vonCerura vinula L. (Lepidoptera). Oecologia 5, 334–346.
Hwang, J.-H., Moon, S.A., Lee, C.H., Byun, M.R., Kim, A.R., Sung, M.K., Park, H.-J., Hwang, E.S., Sung, S.H., Hong, J.-H., 2012. Idesolide inhibits the adipogenic differentiation of mesenchymal cells through the suppression of nitric oxide production. Eur. J. Pharmacol. 685, 218–223.
Julkunen-Tiitto, R., Hakulinen, J., Meier, B., 1994. The response of growth and secondary metabolism to *Melampsora* rusts in field cultivated willow (*Salix*) clones. Acta Hortic. 2, 679–682.
Jung, M.-H., Yoo, J.-M., Kang, Y.-J., Lee, H.W., Kim, S.H., Sung, S.H., Lee, Y.-J., Choi, I., Kim, T.-J., 2010. Idesolide, an isolate of *Idesia polycarpa*, inhibits apoptosis through induction of intracellular heat shock protein 70 in C_2C_{12} muscle cells. Biol. Pharm. Bull. 33, 1063–1066.
Kim, S.H., Sung, S.H., Choi, S.Y., Chung, Y.K., Kim, J., Kim, Y.C., 2005. Idesolide: A new spiro compound from *Idesia polycarpa*. Org. Lett. 7, 3275–3277.
Kim, T.B., Kim, H.W., Lee, M., Lee, H.H., Kim, S.H., Kang, S.K., Sung, S.H., 2014. Isolation and structure elucidation of (−)-idescarparide, a new spiro compound from *Idesia polycarpa*. Tetrahedron Lett. 55, 5447–5449.
Kim, T.W., 1996. The Woody Plants of Korea. Kyohak Press, Seoul, p. 126.
Kumar, M., Rawat, P., Khan, M.F., Tamarkar, A.K., Srivastava, A.K., Arya, K.R., Maurya, R., 2010. Phenolic glycosides from *Dodecadenia grandiflora* and their glucose-6-phosphatase inhibitory activity. Fitoterapia 81, 475–479.
Lee, M., Lee, H.H., Lee, J.-K., Ye, S.-K., Kim, S.H., Sung, S.H., 2013. Anti-adipogenic activity of compounds isolated from *Idesia polycarpa* on 3T3-L1 cells. Bioorg. Med. Chem. Lett. 23, 3170–3174.
Lee, S., 2012. A new megastigmane glucoside from the aerial parts of *Erythronium japonicum*. Nat. Prod. Sci. 18, 166–170.
Massad, T.J., Trumbore, S.E., Ganbat, G., Reichelt, M., Unsicker, S., Boeckler, A., Gleixner, G., Gershenzon, J., Ruehlow, S., 2014. An optimal defense strategy for phenolic glycoside production in *Populus trichocarpa* – isotope labeling demonstrates secondary metabolite production in growing leaves. New Phytol. 203, 607–619.
Moritake, M., Ueda, K., Mori, I., 1987. Two phenazine derivatives, polycartine A and B from *Idesia polycarpa* maxim (Flacourticaceae). Tetrahedron 28, 1425–1426.
Neiman, M., Olson, M.S., Tiffin, P., 2009. Selective histories of poplar protease inhibitors: elevated polymorphism, purifying selection, and positive selection driving divergence of recent duplicates. New Phytol. 183, 740–750.
Otsuka, H., Kamada, K., Yao, M., Yuasa, K., Kida, I., Takeda, Y., 1995. Alangionosides C-F, megastigmane glycosides from *Alangium premnifolium*. Phytochemistry 38, 1431–1435.
Pichette, A., Eftekhari, A., Georges, P., Lavoie, S., Mshvildadze, V., Legault, J., 2010. Cytotoxic phenolic compounds in leaf buds of *Populus tremuloides*. Can. J. Chem. 88, 104–110.
Pinheiro, J., Bates, D., DebRoy, S., Sarkar, D., R Core Team, 2016. nlme: Linear and Nonlinear Mixed Effects Models. R Package Version 3.1-128. http://CRAN.R-project.org/package=nlme.
R Core Team, 2016. R: a Language and Environment for Statistical Computing. R Foundation for Statistical Computing, Vienna, Austria. https://www.R-project.org/.
Robinson, G.S., Ackery, P.R., Kitching, I.J., Beccaloni, G.W., Hernández, L.M., 2010. HOSTS - a Database of the World's Lepidopteran Hostplants. Natural History Museum, London. http://www.nhm.ac.uk/hosts. (Accessed 13 June 2017).
Ruuhola, T., Julkunen-Tiitto, R., Vainiotalo, P., 2003. *In vitro* degradation of willow salicylates. J. Chem. Ecol. 29, 1083–1097.
She, G.-M., Wang, D., Zeng, S.-F., Yang, C.-R., Zhang, Y.-J., 2008. New phenylethanoid glycosides and sugar esters from Ku-Ding-Cha, a herbal tea produced from *Ligustrum purpurascens*. J. Food Sci. 73, C476–C481.
Si, C.-L., Kim, J.-K., Bae, Y.-S., Li, S.-M., 2009. Phenolic compounds in the leaves of *Populus ussuriensis* and their antioxidant activities. Planta Med. 75, 1165–1167.
Therneau, T., 2015. A Package for Survival Analysis in S. Version 2.38. http://CRAN.R-project.org/package=survival.
Thieme, H., 1964. The phenolic glycosides of the Salicaceae. II. Isolation and detection. Pharmazie 19, 471–475.
Wang, J., Constabel, C.P., 2004. Three polyphenol oxidases from hybrid poplar are differentially expressed during development and after wounding and elicitor treatment. Physiol. Plant. 122, 344–353.
Yang, H., Lee, S.H., Sung, S.H., Kim, J., Kim, Y.C., 2013. Neuroprotective compounds from *Salix pseudo-lasiogyne* twigs and their anti-amnesic effects on scopolamine-induced memory deficit in mice. Planta Med. 79, 78–82.
Ye, Y., Tang, X.-S., Chen, F., Tang, L., 2014. Optimization of phenolics extracted from *Idesia polycarpa* defatted fruit residue and its antioxidant and depigmenting activity *in vitro* and *in vivo*. J. Evidence-Based Complement. Altern. Med. 2014, 12.
Zuur, A.F., Ieno, E.N., Walker, N., Saveliev, A.A., Smith, G.M., 2009. Mixed Effects Models and Extensions in Ecology with R. Springer-Verlag, New York.